Tectonophysics 483 (2010) 20–28

Contents lists available at ScienceDirect

Tectonophysics

journal homepage: www.elsevier.com/locate/tecto

Interactions of 3D mantle flow and continental lithosphere near passive margins

R.J. Farrington [a,*], D.R. Stegman [b], L.N. Moresi [a], M. Sandiford [b], D.A. May [c]

[a] School of Mathematical Sciences, Monash University, Clayton, Victoria 3800, Australia
[b] School of Earth Sciences, The University of Melbourne, Carlton, Victoria 3010, Australia
[c] Institute of Geophysics, ETH Zurich, Zurich, 8093, Switzerland

ARTICLE INFO

Article history:
Received 18 February 2009
Received in revised form 2 September 2009
Accepted 9 October 2009
Available online 18 October 2009

Keywords:
Plate driven convection
Small-scale convection
Passive margins
Lithospheric heat flux

ABSTRACT

We investigate the time evolution of 3D numerical models of convection in the upper mantle which incorporate both plate motions and thick continental lithosphere. The resultant flow in the upper mantle is driven by a combination of bottom heated convection and applied shear velocity boundary conditions that represents plate motion. Both the plate velocity and continental lithosphere topography are varied in a way to assess the general influence of 3D geometry as well as a more specific tectonic analogue of the Australian plate. Transient thermal events offshore of the trailing passive margin are observed and include plume migration, boundary layer instability growth at the passive margin and variations in surface heat flux. The geometry and plate velocity both play a significant role in controlling the magnitude and duration of these transient features. In particular, there are large differences between the different models in the oceanic region downstream of the trailing edge of the continent. At near-stationary plate speeds, cold linear downwelling sheets propagate away from the 3D edge of the continent, with regions offshore of the continents central axis localising hot cylindrical upwelling plumes. At very fast plate speeds, the shear flow is dominated by the plate motions. This causes regions neighbouring the trailing edge of the continent to produce broad, hot upwellings and the cold linear sheets to migrate around the continent. At moderate (2 cm/yr) plate speeds, oceanic lithosphere neighbouring the passive margin along the trailing edge of the continent is buffered by cold, downwelling instabilities sinking along the edges of the continental lithosphere. Such neighbouring regions are subjected to larger heat flux than for regions distant to the passive margin, yet also record smaller and less variable vertical surface velocities. These dynamics have implications for volcanism and surface topography, for which 3D aspects play a significant role.

1. Introduction

This study addresses the long-standing hypothesis that continental and oceanic lithosphere operate fundamentally different from each other (Jordan, 1975; Pollack, 1986). In particular, regions of thickened continental lithosphere provide more resistance to heat escaping from the mantle underneath (Jordan, 1975; Pollack, 1986), and provide insulating constant heat flux boundary conditions to the mantle, rather than the constant temperature boundary conditions appropriate for oceanic lithosphere (Lenardic and Kaula, 1995). This insulating effect can lead to heat accumulating beneath stationary continents as the underlying upper mantle gradually warms. Such a situation may be analogous to the separation of the Australian plate from former Gondwanaland. Australia was nearly stationary or very slowly moving for a long period of time prior to around 43 million years ago when fast northward drift commenced (Tikku and Cande, 1999). The continental insulation mechanism has also been proposed to generate very large pools of warmed material underneath supercontinents (Anderson, 1982, 1994). The interaction of large continents with an accumulation of heat within the underlying mantle has been previously investigated with 2D numerical models (Gurnis, 1988; Zhong and Gurnis, 1993; Lowman and Jarvis, 1995) as well as with analogue laboratory models (Guillou and Jaupart, 1995). These early models treat continents as essentially 1D features (rafts on the surface driven by basal tractions from convective flow) that are compositionally buoyant and have higher viscosity which allows them to remain coherent over long (~billion year) timescales. Similarly, rigid caps have been used to investigate the interaction between broad regions of warmed upper mantle and large continents in 3D spherical geometry (Coltice et al., 2007).

The lithosphere underneath continental cratons is also thought to consist of a distinct chemical composition that is both devolatilized (including dehydrated) as well as depleted of its mafic components (Jordan, 1975; Pollack, 1986). These material properties are thought to give it a strong and buoyant character, which helps it maintain long term stability. The thickness of the continental lithosphere varies, but is thickest underneath Archean cratons, in some places in excess of 300 km (i.e. much thicker than typical oceanic lithosphere). We

* Corresponding author.
E-mail address: rebecca.farrington@sci.monash.edu.au (R.J. Farrington).

0040-1951/$ – see front matter © 2009 Elsevier B.V. All rights reserved.
doi:10.1016/j.tecto.2009.10.008

designate the thickness, or depth, of this compositional boundary layer, ΔZ_{CBL}. Later numerical models included for variable continental lithosphere thickness and studied the interactions between 2D continents embedded within the convecting mantle (O'Neill and Moresi, 2003; Cooper et al., 2004). The interactions between compositionally distinct thick continental lithosphere and mantle convection in 3D geometry have received much less attention with recent studies in 3D treating plates as surface velocity boundary conditions (Nettelfield and Lowman, 2007).

One aspect of having variable ΔZ_{CBL} is that large lateral temperature differences can occur between the continental lithosphere and adjacent upper mantle. In the case of a thick continental lithosphere moving at some speed through a passive mantle, a secondary convective flow can be generated in the adjacent mantle along the trailing edge, otherwise referred to as Edge Driven Convection (EDC) (King and Anderson, 1998). EDC describes the time-dependent boundary layer instabilities resulting from lateral temperature variations across large ($\geq$100 km) discontinuous changes of lithospheric thickness. This flow can be considered as a result of 2 different processes, the dynamic flow resulting from thermal buoyancy forces, and the shear flow resulting from plate motions. EDC should be sensitive to the sense of shear beneath moving continents. EDC has been used to explain intraplate volcanism in the absence of deep mantle plumes or extension and is thought to promote both volcanic activity (King, 2005) and anomalous dynamic topography (Shahnas and Pysklywec, 2004). Thus far, numerical models of EDC have been restricted to 2D and do not account for the inherent asymmetry between cold, linear downwelling sheets and hot, point-like cylindrical upwelling plumes as they would normally exist in 3D geometry. This motivates the first suite of numerical models for this study in which we investigate how thick continents interact with varying types of background mantle flows. In particular, we address whether EDC is significantly different in 3D due to the inclusion of the natural asymmetries between the shape of upwellings and downwellings.

The Newer Volcanic Province (NVP) in South Eastern Australia has been proposed as an example of EDC volcanism, with many of the observables required for deep mantle plumes absent in the NVP (King, 2007). Demidjuk et al. (2007) argued that EDC developed on the trailing edge of the continent, with an episodicity of approximately 10 Ma over the past 30 Ma. A recent analysis of surface wave tomography underneath Australia revealed a lithospheric structure that has variations in thickness orthogonal to plate motion (Fishwick et al., 2008). Fishwick et al. (2008) propose a tiered lithospheric structure underneath Australia, as seen in Fig. 1, which shows progressive thinning towards the east, with lithosphere from central Australia having $\Delta Z_{CBL} > 200$ km, followed by $\Delta Z_{CBL} = 150$–200 km, and ending at the coastal section with $\Delta Z_{CBL} \sim 100$ km.

It is not possible to model this type of lithospheric structure in 2D, as the discontinuous steps in ΔZ_{CBL} do not occur in the same plane as the modelled flow. This aspect motivates the second suite of numerical models in this study which investigates the effect of lateral variations of ΔZ_{CBL} in directions only possible in 3D. The 3D geometry used in this study allows the flow from beneath the continent to freely advect past the trailing edge of the continent and interact with the regional 3D convective planform beneath the oceanic lithosphere. This increase in complexity is of interest as 2D flow patterns can become unstable in this more realistic geometry. Planform stability and thermal asymmetries may be important factors in the development and evolution of thermal instabilities along lithospheric discontinuities.

The work presented here, presumes by its initial condition, an insulated mantle underneath a continent. The influence of varying continental lithospheric topography, as well as the velocity with which the continent moves is considered. In particular, we quantify the thermal effects of the trailing passive margin of the continent on the neighbouring oceanic lithosphere. These thermal effects can be quantified through temperature differences in surface boundary layers and have direct consequences on surface observables (dynamic topography, heat flow, surface stresses), with deviations from adiabatic geotherms indicating an excess/deficit of heat. Importantly, these are the first models to employ a 3D geometry to explicitly address instabilities at the trailing edge of fast moving continents and the development of EDC, hypothesized to play a role in generating non-hotspot volcanism.

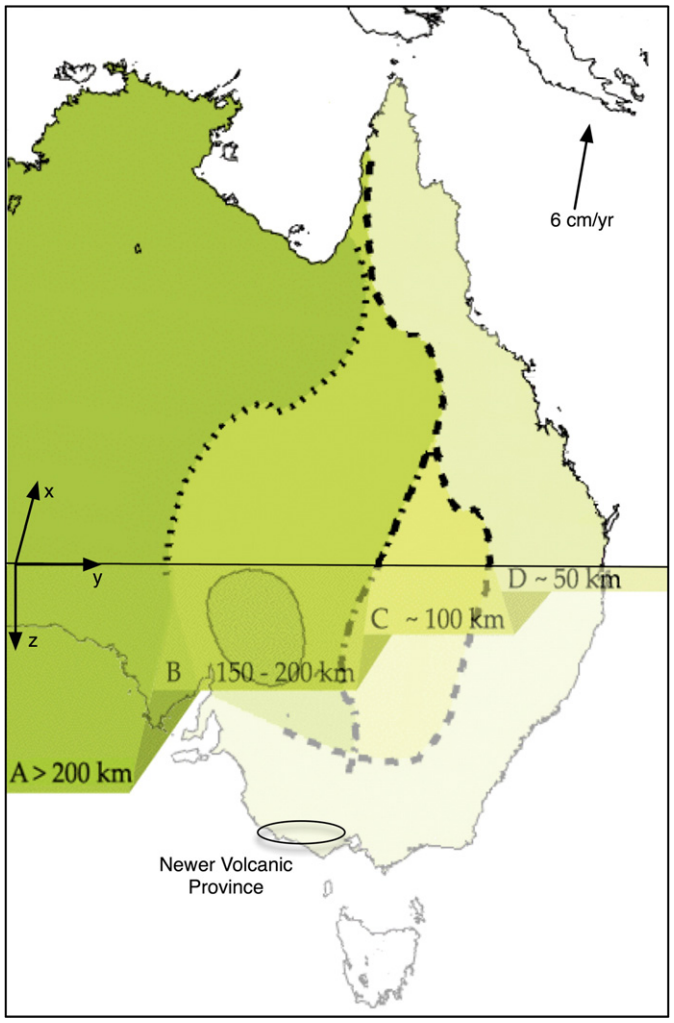

Fig. 1. A map of the Australian continent modified from Fig. 9 of (Fishwick et al. 2008). The location of the Newer Volcanic Provence is shown in South Eastern Australia. The thickness of the lithosphere is shown by colour. Dark green represents regions with a thickness greater than 200 km, light green represents regions between with a thickness between 150 and 200 km, yellow for regions ~100 km thick and cream for regions of ~50 km thick. The 3D tiered structure at depth can be seen in the cross section. The coordinates used within this study and the plate motion vector are shown for reference.

Using a 3D numerical model of mantle convection and building upon previous 2D studies (King and Anderson, 1998; Shahnas and Pysklywec, 2004), this work is a generic study into the effects of a continent with an imposed plate speed on the underlying mantle, encompassing 3D aspects of both mantle convection and lithospheric discontinuities, and its resulting surface expression.

2. Model setup

In this study, a series of 6 models employing 2 continental topographies with 3 plate velocities was used. The goal of this paper is

to determine the relative importance which a 3D geometry has on the surface heat flux variations resulting from both the thermal convection and shearing components of flow present in the upper mantle. We model the interaction between continental lithospheric discontinuities, plate motions and thermal convection within a 3D bottom heated upper mantle. The continent is defined by a compositionally distinct material with a viscosity 10^3 times larger than the reference mantle viscosity of 10^{19} Pa s. The convecting upper mantle is parameterised by a Rayleigh number of 10^6.

The model domain is defined by a Cartesian box of dimensions 5280 km × 5280 km × 660 km (8 × 8 × 1). The continent is defined using either a uniform or a tiered geometry, as shown in Fig. 2. The uniform geometry, with a continent of dimensions 2640 km × 2640 km × 220 km, approximates the size of the Australian continent at 220 km depth (Fishwick et al., 2008). The tiered geometry is defined by the union of 3 layers of thickness 100 km, 150 km and 220 km and width 3216 km, 2400 km and 1236 km respectively, resulting in the tiered form shown in Fig. 2(ii). The symmetry of this model about the *y*-axis is leveraged by placing a free-slip boundary condition through $y = 0$ km. Couette boundary conditions were used to simulate plate motions by applying a velocity in the positive *x*-direction along the bottom boundary with periodic boundary conditions on the side walls and free-slip velocity boundary conditions on the back and front walls. A combination of free-slip and no-slip velocity boundary conditions on the top wall ensure no differential motion along the passive margin.

The initial condition for this model is a thermal statistically steady state mantle (similar to Cooper et al. (2004)) with periodic boundary conditions along the axis of plate motion and prescribed plate speed. The initial thermal steady state was determined using a model with the same geometry, material properties and boundary conditions as outlined above, with the exception of the imposed plate speed. This "no plate velocity" model was evolved in time until the surface heat flux variation was found to be within a tolerance of 1% for a significant period of time (25 Ma).

Table 1
Model parameters including imposed plate speed, continental topography and transient time.

Model	Plate speed	Topography	Transient period
1	0.2 cm/yr	Uniform	–
2	0.2 cm/yr	Tiered	–
3	2.0 cm/yr	Uniform	140 Ma
4	2.0 cm/yr	Tiered	140 Ma
5	20 cm/yr	Uniform	14 Ma
6	20 cm/yr	Tiered	14 Ma

The time used for the 2.0 cm/yr and 20 cm/yr models is the transient period, defined as the time taken for a parcel of mantle to travel along the base of the upper mantle from the centre of the continent, ($x = 0$ km) past the trailing edge to the periodic boundary ($x = 2640$ km). This time is 140 Ma for the 2.0 cm/yr model and 14.0 Ma for the 20 cm/yr model. It was found that the imposed plate speed of 0.2 cm/yr was not large enough to interact with the convective planform of the initial steady state model after 3.4 Ma as shown in Fig. 3(a) and is therefore taken to be equivalent to the steady state model.

The interaction between plate velocity and flow resulting from thermal buoyancy is thought to result in EDC. The thermal buoyancy forces of interest here are a result of instabilities along the lateral temperature variations found across discontinuous changes in ΔZ_{CBL}. Plate velocities within this study are assumed to originate from far field forces, and as such they are imposed as a surface velocity boundary condition. The interaction of these forces with the resulting flow and the presence or absence of EDC is modelled by varying the imposed plate velocity with respect to the velocity resulting from thermal buoyancy forces, i.e. the vertical velocity.

The effect of an imposed plate speed on this initial steady state was studied by defining regimes which were dominated, or balanced, by flow resulting from either the thermal buoyancy or the plate velocity. Three different plate speeds were studied with respect to these regimes (i) flow dominated by thermal buoyancy, (ii) flow balanced between thermal buoyancy and plate velocity (iii) plate velocity dominated. The characteristic plate speed for the three regimes was

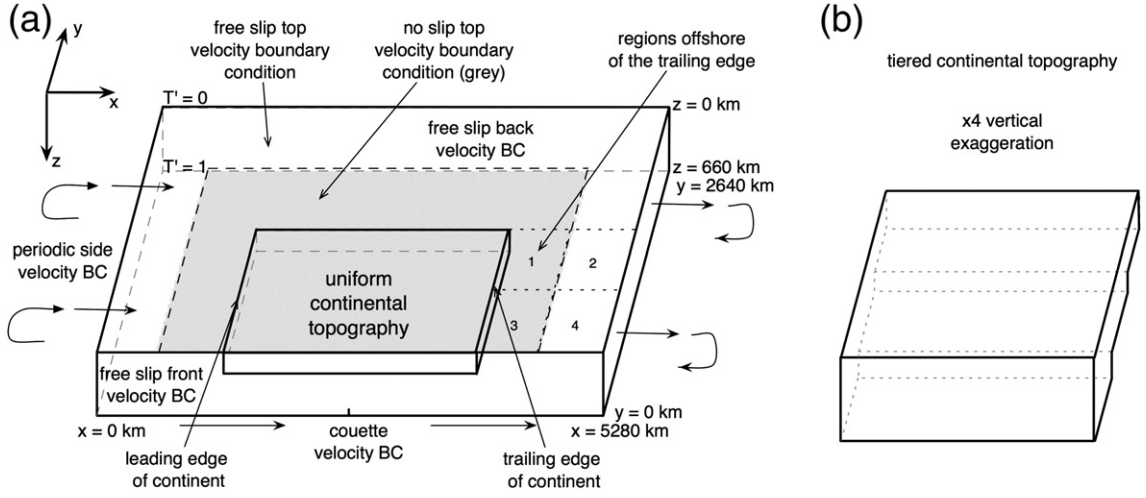

Fig. 2. A schematic of the model setup including coordinate system, domain and continental geometry, velocity and temperature boundary conditions and de-composition of the surface area offshore of the trailing edge of the continent. The origin of the coordinate system is taken to be at the top front left corner of the domain, with *z* representing depth and equal to 0 at the surface. The continent is defined with either (a) block or (b) tiered geometry. The oceanic lithosphere offshore of the trailing edge of the continent has been decomposed into 4 individual regions labelled 1–4, representing regions either adjacent (1,3) or distant (2,4) to the trailing edge passive margin and regions adjacent the central axis (3,4) or distant (1,2) of the continent. The block geometry is defined as a rectangular prism of dimensions 2640 km × 1320 km × 220 km. The tier geometry as shown in (b), with an exaggerated (×4) vertical scale, is defined by the union of 3 rectangular prisms with a constant length of 2640 km, successively smaller depths of 220 km, 150 km and 100 km, and increasing widths of 1236 km, 2400 km and 3216 km respectively. The full domain is a 3D Cartesian box of length 5280 km, width 2640 km and depth 660 km. The symmetry of the continental topography allows for a mirror/free-slip front and back wall velocity boundary condition, cutting the computations required by half. Periodic boundary conditions are used along the left and right wall allowing for the imposed plate motions as for Couette flow. The imposed plate motion is enabled through a prescribed velocity in the positive *x*-direction along the bottom wall. A combination free-slip/no-slip velocity boundary condition is used along the top wall, ensuring no differential motion between the continental and oceanic lithosphere throughout the length of the passive margin. The no-slip region is marked in grey. The temperature is fixed at both the top and bottom wall with a temperature increase across the depth of the domain held constant at ΔT.

defined using the thermal steady state model (driven by only thermal buoyancy forces) as a reference model. From the reference model we computed the RMS value of the vertical component of velocity to obtain a reference speed of 2 cm/yr. From this, we selected the following imposed plate speed for each of the three regimes (i) 0.2 cm/yr, representing thermal buoyancy dominated flow (ii) 2 cm/yr, allowing flow produced by thermal buoyancy and plate velocity of equivalent magnitude to interact and (iii) 20 cm/yr, producing plate velocity (shear) dominated flow.

The models were run for the length of time required to investigate the transient thermal state of the system. This time was defined as the time required for a parcel of mantle to travel from beneath the centre of the continent, past the trailing edge of the continent to the right wall boundary, through half of the domain in the x-direction. This transient time is dependent on the applied plate velocity and differs for the three imposed plate speeds as outlined in Table 1. This model was solved using the Finite-Element Particle-In-Cell software package Underworld (Moresi et al., 2007) utilising only the finite-element

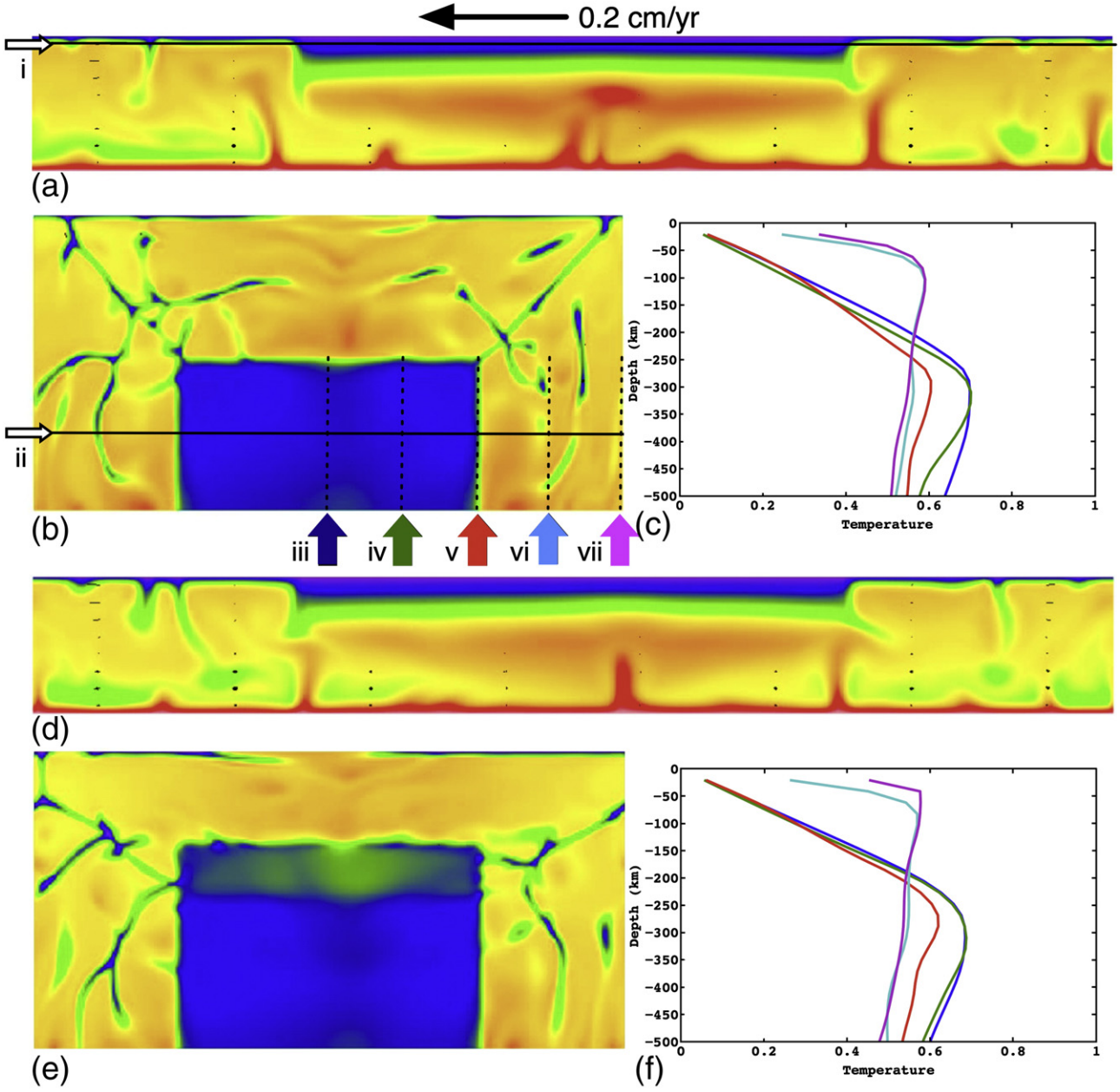

Fig. 3. Simulation results for a plate speed of 0.2 cm/yr (models 1 and 2 in Table 1) taken at 3.4 Ma after the initiation of plate motion and are representative of the pattern of instability growth seen throughout the length of the model. The direction and magnitude of plate motion is indicated by the arrow at the top centre of the figure. (a) Temperature field of the block continental topography for a cross section taken at $y = 660$ km. Cold temperatures are represented with blue, hot with red. The line and arrow marked (i) indicates the location of the cross section shown in (b). (b) Planform of the temperature field for a cross section taken at 66 km depth for the block continental topography. The line and arrow marked (ii) indicates the location of the cross section shown in (a). The coloured arrows numbered (iii) to (vii) indicate the location of the geotherms shown in (c). These geotherms are taken as an average value with depth across only half the width of the domain, as outlined by the dashed lines at each coloured arrow. As an example, the blue arrow marked (iii) corresponds to the blue geotherm in (c) and is calculated using the average temperature with depth at $x = 2640$ km across the width from 0 km $\leq y \leq$ 1320 km. (c) Geotherms found beneath and along the trailing edge of the continent and beneath the oceanic lithosphere within the downstream region of the domain, are defined by the dashed rectangle in (b). Geotherms were taken at $x = 2640$ km (blue), 3300 km (green), 3960 km (red), 4620 km (aqua) and 5280 km (magenta). (d)–(f) as for (a)–(c) with the tiered continental topography.

components of the package. The element resolution used was 25 km in the horizontal direction and 18.75 km in the vertical direction. The velocity was scaled to the current surface RMS velocity for Earth found to be 3.7 cm/yr in the no-net-rotation reference frame taken from Table 2a of Wu et al. (2008).

3. Results

3.1. Buoyancy dominated flow

Fig. 3 details results for a plate speed of 0.2 cm/yr taken at 3.4 Ma after the initiation of plate motion. Fig. 3(a) shows hot material pooling beneath an insulating continent with small-scale instabilities at lithospheric discontinuities. Small-scale flow along the leading edge of the passive margin (left hand side) is shown to act as an anchor point for downwellings directing flow deeper into the mantle. Thermal plumes rising from the base of the upper mantle beneath the trailing edge of the passive margin (right hand side) perturbs the instability, directing flow upwards beneath the oceanic lithosphere.

Fig. 3(b) shows the convection planform through the temperature field at a depth of 66 km, indicating that the inherent symmetry of the reference model is not broken with a plate speed of 0.2 cm/yr. The heat flux and velocity RMS also remain the same as that found in the reference model. This suggests that a low plate speed has a negligible effect on the initial condition and can therefore be considered equivalent to the steady state reference model. Hot upwelling material is concentrated offshore of the central continental regions, both along and perpendicular to the axis of plate motion. Cold downwelling sheets are focused offshore of the passive margin radiating from the continental edges. The cold downwellings continuously migrate away from the continent towards the cold sheets which persist throughout the length of the simulation.

Fig. 3(c) shows a conductive geotherm observed at 250 km depth within the continental thermal lithosphere for $x = 2640$ km (blue) and $x = 3300$ km (green), with the temperature differential across the

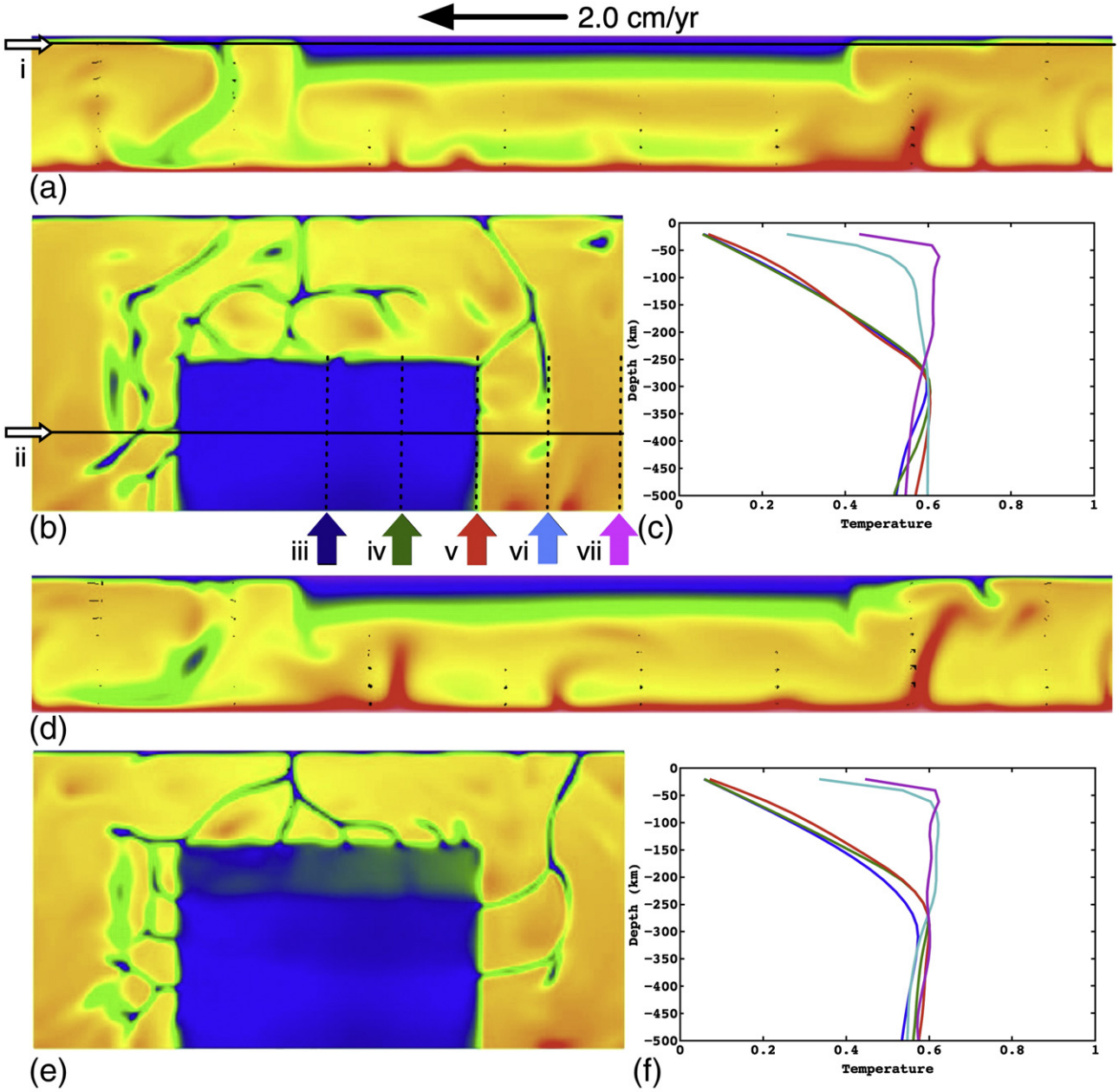

Fig. 4. Simulation results for plate speeds of 2 cm/yr (models 3 and 4) at a time of 140 Ma from the initiation of plate motion as for Fig. 3.

thermal boundary layer (ΔT_{BL}) being 0.7 of the temperature differential across the upper mantle (ΔT) and extending to a depth of 320 km. The oceanic thermal lithosphere (aqua, magenta) persists to 100 km depth with $\Delta T_{BL} = 0.59\Delta T$.

Fig. 3(d) shows the cross section of the temperature field for the tiered continental topography through $y = 660$ km with lithospheric discontinuities again seen to anchor downwellings. Downwellings focused at the continental discontinuities propagate away perpendicular to the passive margin. Upwellings are focused offshore of the central regions of the continent in both the x- and y-axis. The sub-continental geotherms of the tiered topography as shown in Fig. 3(f) indicate that the depth of the thermal lithosphere is the same for both continental topographies. The temperature drop across this conductive region is however smaller, with $\Delta T_{BL} = 0.68\Delta T$ for the continental and $\Delta T_{BL} = 0.57\Delta T$ for the oceanic lithosphere.

3.2. Buoyancy and shear flow balanced

Fig. 4(a) taken 140 Ma after the initiation of a plate velocity of 2.0 cm/yr shows the hot insulated mantle, located originally beneath the continent, swept past the trailing edge of the passive margin resulting in a large scale thermal upwelling offshore. Lateral temperature differences along the passive margin result in time-dependent boundary layer instabilities forming an EDC cell. The passive margin at the leading edge of the continent shows a concentration of cold downwellings. The downwelling present at this passive margin blocks the movement of upwelling plumes directing flow deep into the upper mantle cooling the upstream portion of the sub-continental mantle.

A plate speed of 2.0 cm/yr is sufficient to disrupt the symmetry of the convection planform as shown in Fig. 4(b). Numerous cold downwellings are located offshore of the leading edge of the continental margin with hot upwellings focused offshore of the trailing edge along the central axis. Two distinct upwellings can be seen downstream at a distance of approximately 300 km and 800 km from the passive margin. The transportation of the insulated sub-continental mantle past the trailing edge of the passive margin results in a decrease in ΔT_{BL} to $0.6\Delta T$ as shown in Fig. 4(c) for the continental thermal lithosphere compared to the previous small plate speed results. A variation in the depth and ΔT_{BL} of the oceanic thermal lithosphere can also be seen with temperature gradients increasing to 100 km depth at (iv) but only 60 km at (vii).

The tiered continental topography, shown in Fig. 4(d), results in time-dependent boundary layer instabilities along the passive margins. These instabilities also interact with the downwelling sheets radiating from lateral discontinuities within the passive margin, Fig. 4(e). In the case of the trailing edge passive margin this results in a larger downwelling mass as seen in Fig. 5 when compared to the uniform continental topography.

As shown in Fig. 4(e), the interaction with shear flow resulting from the plate motion elongates downwelling sheets in comparison to those found for the slower plate speed. Hot upwellings are again focused along the central axis of the continent downstream of the passive margin. The sub-oceanic geotherms shown in Fig. 4(f) again show a thermal lithosphere depth of $\Delta T_{BL} = 0.6\Delta T$ in both locations (vi, vii).

Focusing on the area offshore of the trailing edge of the continent only, the evolution of the surface heat flux within different regions (outlined in Fig. 2) is shown in Fig. 5. Initial values for these regions indicate the partitioning of the total initial surface heat flux within the total downstream region. The regions adjacent to the passive margin (red and green) have the largest heat flux, being approximately 50% higher than the average steady state value. The regions distant to the passive margin maintain a smaller heat flux, being 50% smaller than the average steady state value for the total area.

Within the regions neighbouring the trailing edge of the continent (red and greed) the heat flux shows some oscillations. Within the central region (green) for the first 40 Ma, then between 90 Ma and 120 Ma a periodicity between 12 Ma and 15 Ma is observed. Both regions at a distant to the passive margin show large oscillations throughout the evolution of the model.

The evolution of the near surface vertical velocity for both the uniform and tiered continental topographies across different regions within the area offshore of the trailing edge of the continent is shown in Fig. 6. The vertical velocity for the adjacent regions (red and green) remains relatively steady, showing a consistent increase with time. However these regions again show an oscillation that can be observed at a period between 12 Ma and 15 Ma. The distant regions (blue and

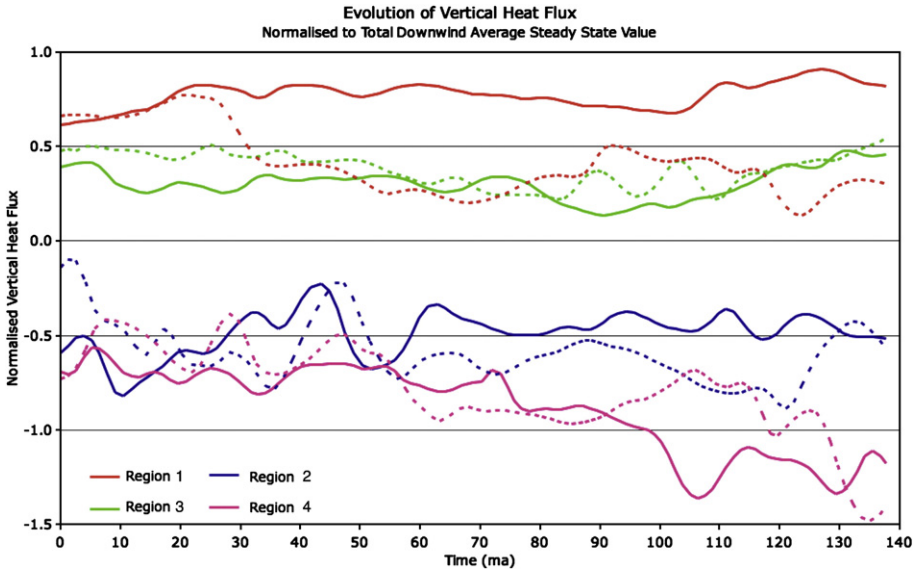

Fig. 5. Evolution of the normalised vertical heat flux with time (Ma) for both a uniform (solid line) and tiered (dotted line) continental topography within the downstream regions at a depth of 50 km. The downstream domain is decomposed into four regions using the location of the central trailing edge of the passive margin as a reference outlined in Fig. 2. The vertical heat flux values are averaged across the surface elements within the region and then normalised for the steady state surface heat flux for the entire downstream domain. Red: 1320 km $< x <$ 1980 km, 0 km $< z <$ 66 km, region (1). Green: 1980 km $< x <$ 2640 km, 0 $< z <$ 660 km, region (2). Blue: 1320 km $< x <$ 1980 km, 660 km $< z <$ 1320 km, region (3). Magenta: 1980 km $< x <$ 2640 km, 660 km $< z <$ 1320 km, region (4).

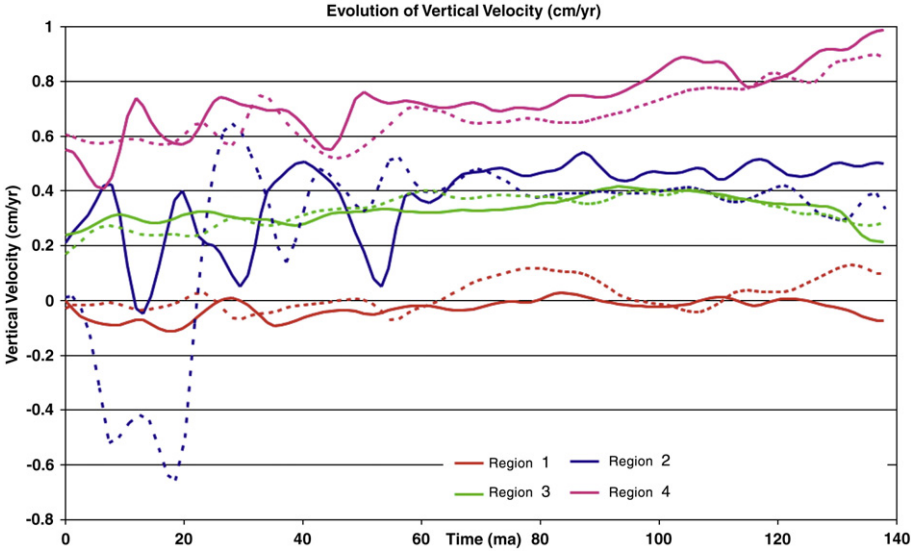

Fig. 6. Evolution of the vertical velocity (cm/yr) with time (Ma) for both a uniform (solid) and tiered (dotted) continental topography for the downstream region at a depth of 50 km. The downstream domain is decomposed into four regions using the location of the central passive margin as a reference, outlined in Fig. 2. Vertical velocity is averaged across the individual regions. Red: 1320 km $< x <$ 1980 km, 0 km $< z <$ 66 km, region (1). Green: 1980 km $< x <$ 2640 km, 0 km $< z <$ 660 km, region (2). Blue: 1320 km $< x <$ 1980 km, 660 km $< z <$ 1320 km, region (3). Magenta: 1980 km $< x <$ 2640 km, 660 km $< z <$ 1320 km, region (4).

magenta) show large fluctuations throughout the evolution. The region distant to the trailing edge passive margin for the uniform topography (solid, blue and magenta) fluctuates with a similar period (20 Ma), but differs in magnitude and phase throughout the first 60 Ma. The trends of the tiered (dotted) continental topography between the distant outer regions and those central to the passive margin differ. The distant outer (blue) region maintains an oscillation with a period of approximately 15 Ma for the first 80 Ma of plate motion. The amplitude of the oscillation then smoothly decays to a steady 0.4 cm/yr at 80 Ma and the periodicity breaks down, at 110 Ma an oscillation of period ~15 Ma returns. The tiered distant central region (magenta) follows a trend similar to its corresponding uniform model.

3.3. Shear dominated flow

The temperature field with a plate speed of 20 cm/yr at a time of 14 Ma after the initiation of plate motion for the uniform and tiered continental topography is shown in Fig. 7(a) and (d) respectively. Shear velocity resulting from plate motion dominates the flow, inhibiting plumes rising from the base of the upper mantle and elongating the cold downwelling sheets. For the uniform topography this results in continuous large scale upwellings offshore of the trailing edge of the continent as shown in Fig. 7(b). The elongated cool downwellings seen at lateral continental discontinuities for the tiered topography (see Fig. 7(e)) focus the thermal upwellings past the trailing edge of the continent along the central axis (with plate motion). In Fig. 7(d), boundary layer instabilities along all passive margins are seen to be 'pinched' by the shear flow, directing upwellings in a downstream direction, with respect to the continent at both the leading and trailing edge of the continent. The increased cold downwellings present offshore of the trailing edge for the tiered topography result in a larger boundary layer instability along this passive margin, directing upwelling flow further offshore of the passive margin.

The shear flow has organised cold plumes originally radiating from the continental edges around the continent. As a consequence the sub-continental ΔT_{BL} remains large as shown in Fig. 7(c) and (e) in comparison to the moderate plate speed seen in Fig. 4(b) where the continent overruns the cold downwellings originally located upstream to the continent. The sub-oceanic thermal lithosphere has the greatest ΔT_{BL} of all plate speeds with both locations and topographies in excess of $0.63\Delta T$.

4. Discussion

The increased insulating effects of a deep continental lithosphere (Grigne et al., 2007) and its effect on the large scale flow (Guillou and Jaupart, 1995) can be seen in Fig. 3 with heat pooling within the sub-continental mantle. When advected at sufficient plate speeds the insulated mantle can be swept downstream, increasing instabilities at ΔZ_{CBL} discontinuities and focusing upwellings offshore of the trailing edge of the continent as seen in Fig. 4. Density driven thermal boundary layer instabilities at ΔZ_{CBL} direct flow for all plate speeds. At small plate speeds, the flow is directed downward into the upper mantle, with lateral flow only present when instabilities at the ΔZ_{CBL} are perturbed by upwelling hot plumes. This flow can be considered as a reference model with flow advected by thermal buoyancy forces alone. At moderate plate speeds, with flow caused by both thermal buoyancy and plate motions, instabilities at the passive margin direct upwelling flow past the trailing edge of the continent. The sub-continental mantle cools as the hot material is advected by shearing as seen in Fig. 4(a) and (d). Plate speeds exceeding those seen on Earth result in large thermal upwellings downstream of the passive margin, Fig. 7(c) and (e). The original hot sub-continental mantle remains cool, as linear downwelling sheets are directed around the fast moving continent.

The inherent asymmetry between cold sheets and hot plumes within the 3D geometry modifies both the lateral length scale of the instabilities and the localisation of the resulting heat flow. The insulated mantle advected past the trailing edge of the continent and upwelled offshore is focused along the central axis of the continent, at a distance from the continental discontinuities (Fig. 4(a)). O'Neill and Moresi (2003) found downwellings with a 2D two-tiered continental topography are focused at lithospheric discontinuities. With the introduction of continental discontinuities in the third dimension, the localisation of multiple downwelling sheets can be seen. While this is observed for both continental geometries, the effect is greater for the tiered geometry (with multiple ΔZ_{CBL} discontinuities) as observed in the differing heat flux for continental topography adjacent to the

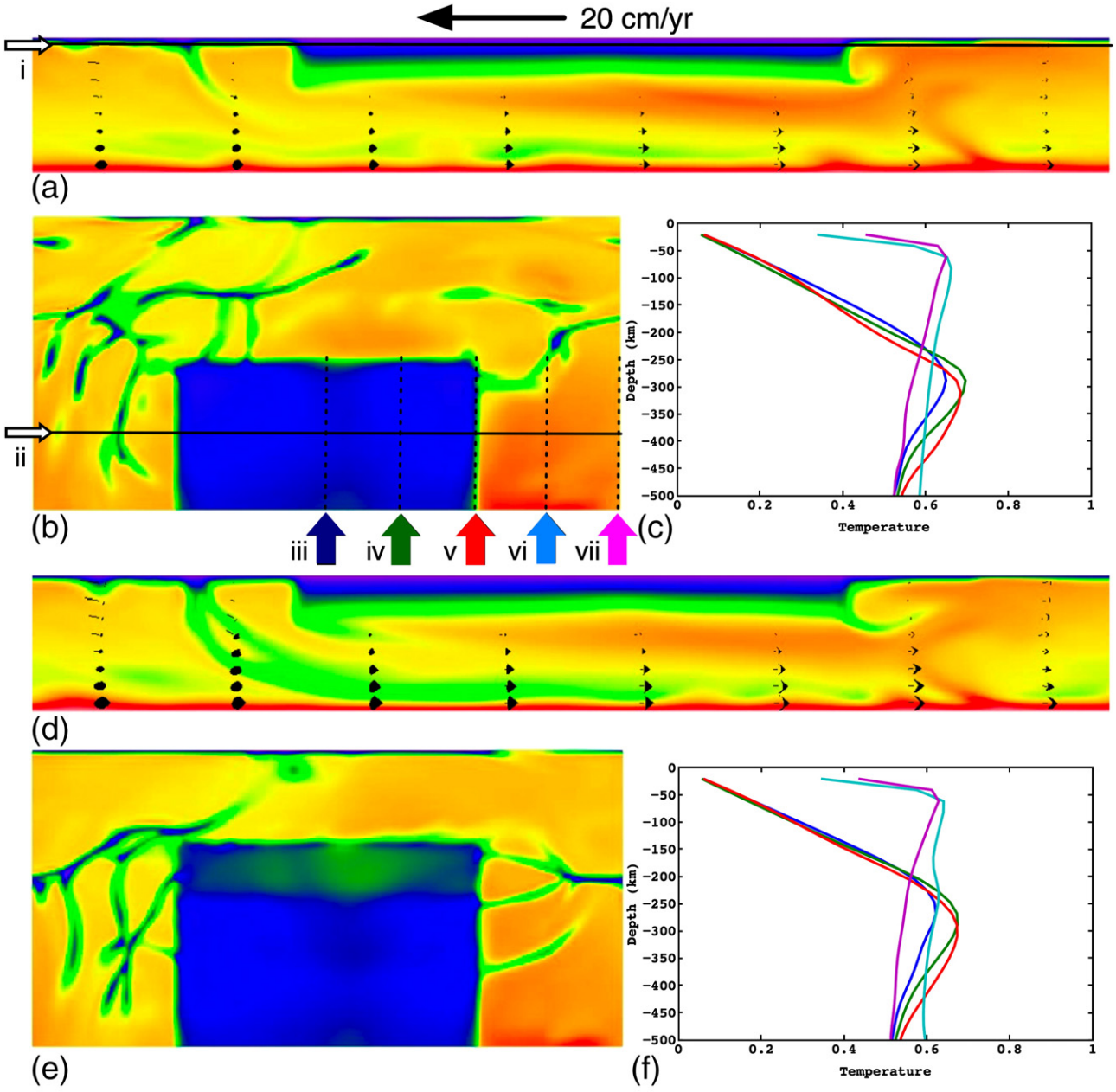

Fig. 7. Simulation results for plate speeds of 20 cm/yr (models 5 and 6) at a time of 14 Ma from the initiation of plate motion as for Fig. 3.

passive margin near the multiple ΔZ_{CBL} discontinuities, Fig. 5. The variation in heat flux with distance from ΔZ_{CBL} discontinuities may be a key factor in the identification of EDC, with lateral variations in volcanic activity within regions offshore of the trailing edge of the continent. However more advanced models, taking into account a non-linear mantle and surface observables are required before these results can imply a stronger connection.

Heat flux and velocity trends for the regions neighbouring the trailing edge passive margin show less variation when compared to those at a distant. These steady regions indicate that the flow resulting from boundary layer instabilities at ΔZ_{CBL} discontinuities acts as an anchor, buffering nearby regions from the large scale convection present within these regional models. The largest changes both in periodicity and long term smoothed trends occur in the distant regions, as a consequence of the continual migration of large scale features across these regions. The oceanic lithosphere next to the trailing edge passive margin measures the greatest heat flux as shown in Fig. 5. However as seen in Fig. 6, the vertical velocity within these regions is smaller than the more distant regions, thus buffering the region from the cooling effect of the larger scale mantle flow. When viewed in the 3D regional setting, EDC can dominate the flow in the local (small/sub-upper mantle) length scale and may provide a mechanism for the mixing and melting of material originally beneath the continental craton. However a small frequency signal, which may indicate a local increase in heat flux or vertical velocity, could be smoothed out by the averaging used in this study. A potential example of this is the hot plumes discussed for both Fig. 4(b) and (e) along the central axis of the continent along the direction of plate motion.

Continental lithosphere at a velocity through the mantle can have an influence on continental geotherms (O'Neill and Moresi, 2003; Michaut and Jaupart, 2004), sub-continental geotherms (Cooper et al., 2004) and as shown here sub-oceanic geotherms. Results from plate velocities of 0.2 cm/yr, taken here to represent negligible plate velocity, show geotherms as expected for oceanic regions with large temperature drops concentrated within the shallow lithosphere. This is also true for continental regions with geotherms registering a thick

conducting lithosphere with a constant temperature differential across the depth of the continent and into the continental thermal boundary layer. However with an increase in plate velocity to 2.0 cm/yr, an increase in the temperature drop across the oceanic boundary layer is seen. This indicates the potential for super-adiabatic geotherms and therefore the occurrence of thermally driven events within this region. Conversely, the temperature drop across the continental boundary decreases, indicating a cooling of the material below the continent. This study is restricted to the investigation of interactions between the upper mantle and ΔZ_{CBL} discontinuities occurring during the transition from a stationary continent to a continent in motion. However, this cooling of the sub-continental mantle may have a significant effect on the instabilities forming along ΔZ_{CBL} discontinuities as it approaches steady state, potentially decreasing the magnitude of these instabilities.

Depending on plate velocity the insulated sub-continental mantle can be advected past the trailing edge of the continent interacting with regional mantle convection. At sufficient plate speeds EDC can form, however the surface expression of this secondary mode of convection is undetermined within this study. Demidjuk et al. (2007) found the Newer Volcanic Provence in Australia has a circulation timescale of order 10 Ma for material travelling from the base of the cratonic lithosphere underneath the Australian continent to the surface via volcanic activity. This timescale was also implicated by the presence of further volcanism within this region dating to between 19 and 30 Ma. In this study, with a plate speed of 2.0 cm/yr, we identify a periodicity of between 12 Ma and 15 Ma for both the heat flux and vertical velocity within the region adjacent to the trailing edge of the continent—the proposed location of EDC. The plate speed of 2 cm/yr used for this study is smaller than that of the Australian plate as it was chosen in order to illuminate the interaction between competing forces not in reference to a particular plate velocity. The Australian plate is moving at over 6 cm/yr (O'Neill et al., 2005) and is therefore within the regime where buoyancy driven thermal velocities are of equivalent magnitude to those of the plate velocity. The factor of 3 difference between the model and the actual velocity of the Australian continent might reduce the periodicity found in the models, becoming closer to the observed 10 Ma timescale.

4.1. Future directions

The side wall velocity boundary conditions used in this model being periodic are sufficient for studying the initial, transient stage when a plate begins moving. In order to study the potential for longer lived steady state EDC, in the absence of an initially insulated sub-continental mantle, inflow/heat flux boundary conditions would be a requirement.

The isoviscous rheology used here allows for a first order approximation of the Earth's mantle. In order to study EDC in more detail and with reference to specific surface expressions, a non-linear rheology, with temperature and strain rate dependence is required. The inclusion of a more complex and realistic rheology may affect the dynamics of the EDC outlined above. Using an isoviscous mantle is however an important step in understanding the interaction between the passive and active flow, particularly with the more complicated 3D convection planform and continental topographies included in this study.

5. Conclusion

Boundary layer instabilities are observed to act as anchors for small-scale flow at passive margins when compositional and thermal discontinuities exist at depth within the upper mantle. The time-dependent nature of these instabilities can be magnified and directed as a function of plate velocity. At sufficient speeds the thermally insulated sub-continental mantle can be swept downstream resulting in hot upwellings downstream of a passive margin. At Earth-like speeds, regional variations indicate that flow anchored by continental discontinuities buffers the region adjacent to the trailing edge of the passive margin, resulting in smoother vertical velocities and heat flux within these areas, with an observed periodicity between 12 Ma and 15 Ma. Fluctuations in surface heat flux are greater for the regions distant to the passive margin, however the heat flux is largest within regions neighbouring the margin. In order to study these phenomena in detail a more realistic mantle rheology is required.

Acknowledgments

Software was provided by AuScope Ltd, funded under the National Collaborative Research Infrastructure Strategy (NCRIS) an Australian Commonwealth Government Programme. Computational resources were provided by the National Computational Infrastructure National Facility. This research was supported under Australian Research Council's Discovery Projects funding scheme (project number DP066325).

References

Anderson, D., 1982. Hotspots, polar wander, Mesozoic convection and the geoid Jun Nature 297, 391–393.
Anderson, D., Jan 1994. Superplumes or supercontinents. Geology 22, 39–42.
Coltice, N., Phillips, B., Bertrand, H., Ricard, Y., Rey, P., 2007. Global warming of the mantle at the origin of flood basalts over supercontinents. Geology 35, 391–394.
Cooper, C.M., Lenardic, A., Moresi, L., 2004. The thermal structure of stable continental lithosphere within a dynamic mantle. Earth and Planetary Science Letters 222, 807–817.
Demidjuk, Z., Turner, S., Sandiford, M., George, R., Foden, J., Etheridge, M., 2007. U-series isotope and geodynamic constraints on mantle melting processes beneath the Newer Volcanic Province in South Australia SEP 30 Earth and Planetary Science Letters 261 (3–4), 517–533.
Fishwick, S., Heintz, M., Kennett, B.L.N., Reading, A.M., Yoshizawa, K., 2008. Steps in lithospheric thickness within eastern Australia, evidence from surface wave tomography. Tectonics 27 (4).
Grigne, C., Labrosse, S., Tackley, P.J., 2007. Convection under a lid of finite conductivity: Heat flux scaling and convection under a lid of finite conductivity: Heat flux scaling and application to continents. Journal of Geophysical Research 112.
Guillou, L., Jaupart, C., 1995. On the effect of continents on mantle convection. Journal of Geophysical Research B: Solid Earth 100, 24217–24238.
Gurnis, M., 1988. Large-scale mantle convection and the aggregation and dispersal of supercontinents. Nature 332, 695–699.
Jordan, T., 1975. The continental tectosphere. Reviews of Geophysics and Space Physics 13, 1–12.
King, S., 2005. Archean cratons and mantle dynamics. Earth and Planetary Science Letters 234, 1–14.
King, S., Anderson, D., 1998. Edge-driven convection AUG Earth and Planetary Science Letters 160 (3–4), 289–296.
King, S.D., 2007. Hotspots and edge-driven convection. Geology 35 (3), 223–226.
Lenardic, A., Kaula, W., Dec 1995. Mantle dynamics and the heat-flow into the Earths continents. Nature 378, 709–711.
Lowman, J., Jarvis, G.T., 1995. Mantle convection models of continental collisions and breakup incorporating finite thickness plates. Physics of the Earth and Planetary Interiors 88, 53–68.
Michaut, C., Jaupart, C., 2004. Nonequilibrium temperatures and cooling rates in thick continental lithosphere. Geophysical Research Letters 31.
Moresi, L., Quenette, S., Lemiale, V., Mériaux, C., Appelbe, B., Mühlhaus, H.-B., 2007. Computational approaches to studying non-linear dynamics of the crust and mantle. Physics of the Earth and Planetary Interiors 163, 69–82.
Nettelfield, D., Lowman, J., 2007. The influence of plate-like surface motion on upwelling dynamics in numerical mantle convection models. Physics of the Earth and Planetary Interiors 161, 184–201.
O'Neill, C., Müller, R.D., Steinberger, B., 2005. On the uncertainties in hot spot reconstructions and the significance of moving hot spot reference frames. Geochemistry, Geophysics, Geosystems 6.
O'Neill, C.J., Moresi, L., 2003. How long can diamonds remain stable in the continental lithosphere? Earth and Planetary Science Letters 213, 43–52.
Pollack, H., 1986. Cratonization and thermal evolution of the mantle Oct. Earth and Planetary Science Letters 80, 175–182.
Shahnas, M., Pysklywec, R., 2004. Anomalous topography in the western Atlantic caused by edge-driven convection SEP 30 Geophysical Research Letters 31 (18).
Tikku, A., Cande, S., 1999. The oldest magnetic anomalies in the Australian–Antarctic basin: are they isochrons? Journal of Geophysical Research 104, 661–677.
Wu, B., Conrad, C., Heuret, A., Lithgow-Bertelloni, C., Lallemand, S., 2008. Reconciling strong slab pull and weak plate bending: the plate motion constraint on the strength of mantle slabs. Earth and Planetary Science Letters 272, 412–421.
Zhong, S., Gurnis, M., 1993. Dynamic feedback between an non-subducting raft and thermal convection. Journal of Geophysical Research 98, 12219–12232.